



# Characterizing the original ejection velocity field of the Koronis family

V. Carruba<sup>a,b,\*</sup>, D. Nesvorný<sup>b</sup>, S. Aljbaae<sup>a</sup>

<sup>a</sup> *Univ. Estadual Paulista - UNESP, Grupo de Dinâmica Orbital & Planetologia, Guaratinguetá, CEP 12516-410, SP, Brazil*

<sup>b</sup> *Department of Space Studies, Southwest Space Research Institute, 1050 Walnut St., Boulder, CO 80302, USA*

---

## Abstract

An asteroid family forms as a result of a collision between an impactor and a parent body. The fragments with ejection speeds higher than the escape velocity from the parent body can escape its gravitational pull. The cloud of escaping debris can be identified by the proximity of orbits in proper element, or frequency, domains. Obtaining estimates of the original ejection speed can provide valuable constraints on the physical processes occurring during collision, and used to calibrate impact simulations. Unfortunately, proper elements of asteroids families are modified by gravitational and non-gravitational effects, such as resonant dynamics, encounters with massive bodies, and the Yarkovsky effect, such that information on the original ejection speeds is often lost, especially for older, more evolved families.

It has been recently suggested that the distribution in proper inclination of the Koronis family may have not been significantly perturbed by local dynamics, and that information on the component of the ejection velocity that is perpendicular to the orbital plane ( $v_W$ ), may still be available, at least in part. In this work we estimate the magnitude of the original ejection velocity speeds of Koronis members using the observed distribution in proper eccentricity and inclination, and accounting for the spread caused by dynamical effects. Our results show that i) the spread in the original ejection speeds is, to within a 15% error, inversely proportional to the fragment size, and ii) the minimum ejection velocity is of the order of 50 m/s, with larger values possible depending on the orbital configuration at the break-up.

© 2011 Elsevier Ltd. All rights reserved

*Keywords:* Celestial mechanics; asteroids; asteroids, dynamics.

---

## 1. Introduction

Asteroid families are the outcome of high-velocity collisions between asteroids. If the fragments of collisions have speeds exceeding the escape velocity from the parent body, they may be ejected and form a swarm around the main body (or, in case of a catastrophic collision, around the family barycenter). Since the terminal ejection speeds are only a fraction of the orbital speed of most main belt bodies, the fragments are not ejected far and may be identified by the fact that they form clusters in the domain of proper elements ( $a, e, \sin(i)$ ) (or proper frequencies

---

\*Corresponding author

*Email address:* [vcarruba@feg.unesp.br](mailto:vcarruba@feg.unesp.br) (V. Carruba)

$(n, g, g + s)$  (see Knežević and Milani (2000) for a description of the methods used to obtain proper elements and frequencies), with  $a$ ,  $e$  and  $i$  being the asteroids proper semi-major axis, eccentricity, and inclination, and  $n$ ,  $g$ ,  $s$  being the proper mean-motion, frequency of precession of the longitudes of pericenter, and of the node, respectively (Bendjoya and Zappalà, 2002; Carruba and Michtchenko, 2007).

Theoretically, ejection speeds of asteroid family members could be estimated from the distribution in proper elements  $(a, e, \sin(i))$  using Gauss'equations (Zappalà et al., 1996), provided that both the true anomaly and the argument of perihelion of the family parent body are known (or estimated). In practice, several gravitational and non-gravitational effects, such as resonant dynamics (Morbidelli and Nesvorný, 1999), close encounters with massive asteroids (Carruba et al., 2003), and the Yarkovsky effect (Bottke et al., 2001) can change proper elements of asteroid families, so that information on the original ejection speeds is sometimes lost, especially for older, more dynamically evolved groups.

Recently, however, Carruba and Nesvorný (2015c), based on arguments on the current shape of the distribution in  $\sin(i)$  of the Koronis family, suggested that information on the component of the ejection velocity that is perpendicular to the orbital plane ( $v_W$ ) may still be available for this family, at least in part <sup>1</sup>. In this work we extend the analysis of the previous paper, and try for the first time to obtain estimates of the original spread of the ejection velocity field for the Koronis group, based on the *eccentricity and inclination* distributions, rather than on the semi-major axis one, as previously attempted (Carruba et al., 2015b). By performing long-term simulations of fictitious Koronis members, we were able to evaluate the effect that dynamics may have had on the inclination distribution, and to estimate what the original distribution should have been, so allowing us to obtain a value of the spread in ejection speeds.

This paper is so divided: in Sect. 2 we identify the Koronis family and its halo, and we verify what is the current dispersion of the family in proper  $e$  and  $\sin(i)$ . In Sect. 3 we study the effect that the local dynamics may have had on the orbital evolution of Koronis family members, and determine to which extent the original distribution in  $e$  and  $\sin(i)$  have been preserved. In Sect. 4 we estimate what was the original dispersion of the Koronis family in proper inclination, determine how the spread in original inclination depended on the family members sizes, and estimate what was the magnitude of the family original ejection velocity field. Finally, in Sect. 5 we present our conclusions.

## 2. Family identification

The Koronis family is located in a relatively dynamically quiet region, where, with the exception of the  $3\nu_6 - 2\nu_5 = g + 2g_5 - 3g_6$  secular resonance, a pericenter resonance that mostly modifies asteroid eccentricities, no other major mean-motion or secular resonance exists (Bottke et al., 2001; Carruba et al., 2013; Nesvorný et al., 2015). The long-term dynamics of the Koronis family should therefore had had a minor influence in the spreading in proper  $i$  of members of the family, as we will also further investigate later on in this paper. Despite being a relatively old family (2.65 Gyr at most if one use standard values for the parameters describing the Yarkovsky force (Brož et al., 2013), see Carruba et al. (2015b) and references therein for more detail on this age estimate), the current dispersion in proper  $i$  of Koronis family members could therefore still contain traces of information on the original ejection speeds (Cellino et al., 2004, 2009).

---

<sup>1</sup>Information on the original ejection velocity field could be in principle also obtainable from very young families proper  $e$  and  $i$  distributions, such as for instance the Datura and Lorre clusters. Here however we focus our attention on a relatively old family, to check whatever information may still available for more evolved groups.

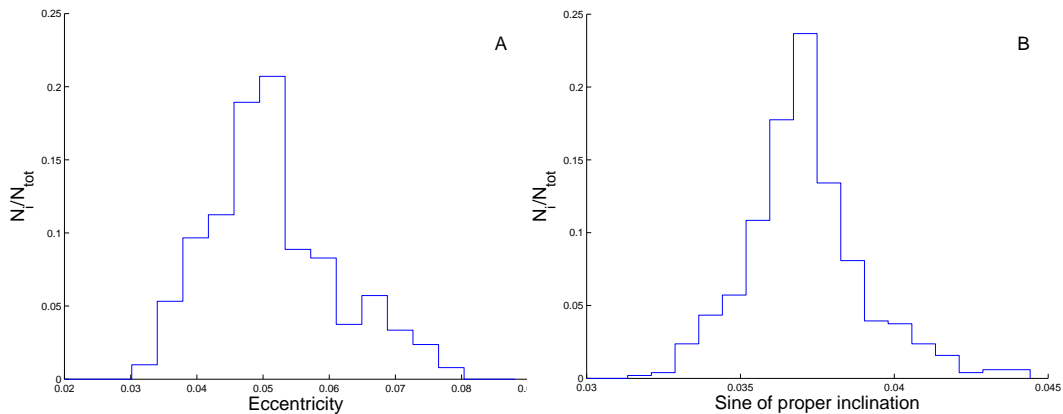


Figure 1: Panel A: histograms of the frequency distribution in proper eccentricity  $e$  for a reduced Koronis family with proper semi-major axis  $a < 2.88$  AU, for objects with  $2 < D < 4$  km ( $D_3$  population). Panel B: similar histograms, but for the distribution in proper sine of inclination  $\sin(i)$ .

To investigate this hypothesis, we first obtained an estimate of the current family members. We used data published in Nesvorný et al. (2015) for the Koronis family using the Hierarchical Clustering Method (Zappalà et al., 1990), and a velocity cutoff of 45 m/s in the  $(a, e, \sin(i))$  domain (see Table 2 in Nesvorný et al. (2015) for further details). Since there are two subfamilies inside the Koronis group, the Karin cluster (Nesvorný et al. (2002, 2006)) and the Koronis 2 family (Molnar and Haegert, 2009), we eliminated these two subgroups from the list of Koronis members. This left us with a sample of 5163 objects, out of the original 5949 members of the whole Koronis and subfamilies sample.

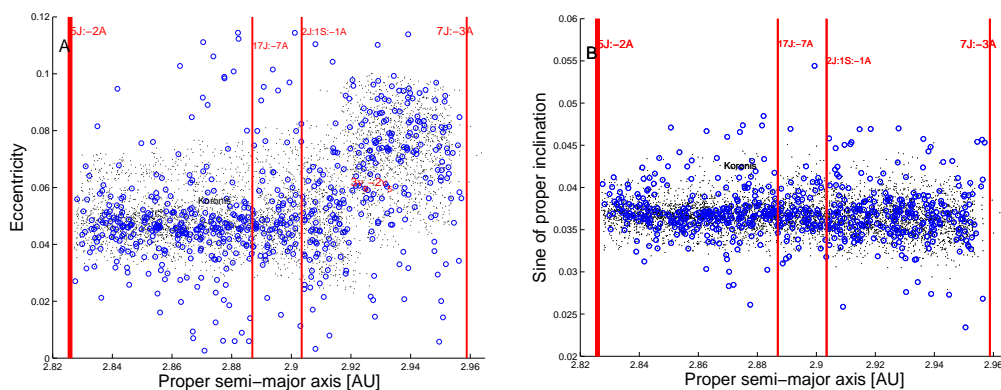
To eliminate possible interlopers, we used the classification method of DeMeo and Carry (2013) that employs Sloan Digital Sky Survey-Moving Object Catalog data, fourth release (SDSS-MOC4 hereafter, Ivezić et al. (2001) to compute  $gri$  slope and  $z' - i'$  colors, and data from the three major photometric/spectroscopic surveys: ECAS, Eight-Color Asteroid Analysis, Zellner et al. (1985); Tholen (1989), SMASS, Small Main Belt Spectroscopic Survey, Xu et al. (1995); Bus and Binzel (2002a,b), and S3OS2, Small Solar System Objects Spectroscopic Survey, Lazzaro et al. (2004). We obtained 896 observations in the SDSS-MOC4 catalog, and taxonomical information for 507 individual asteroids in the revised Koronis family (i.e., the Koronis family, less the two sub-families of Karin and Koronis 2). We found 3 C-type, 8 D-type, 29 X-type, 109 L-type, 259 S-type, 98 K-type, and 1 A-type object, respectively.

Our results confirm the analysis of Binzel et al. (1993); Carruba et al. (2013, 2015b): the Koronis family is an S-complex group, with a small percentage (40 objects, 7.9% of the available sample) of C-complex interlopers. This is further confirmed by the values of geometric albedos  $p_V$  from the WISE mission (Masiero et al., 2012) for local asteroids. Out of the 507 asteroids with taxonomical information, 284 have data in the WISE dataset. Only one object (25285 1998 WB7) has a value of  $p_V$  less than 0.1, normally associated with C-complex asteroids, and could be considered an albedo interloper.

After eliminating three more objects outside the Yarkovsky isolines of the Koronis family (see Nesvorný et al. (2015), sect. 4), we were left with a sample of 5118 asteroids. Fig. 1, panel A, displays a histogram of the frequency distribution in proper  $e$  for a reduced Koronis family with proper  $a < 2.88$  AU (to avoid including asteroids that crossed the  $g + 2g_5 - 3g_6$  secular resonance and other mean-motion resonances, see next section for a more in depth discussion of

Table 1: Number of objects, median, and standard deviation for the different size populations of the 5118 Koronis sample in proper  $e$  and  $\sin(i)$ .

Population	# of objects	Median $e$	Std( $e$ )
All	2037	0.0489	0.0085
$D > 20$ km	10	0.0471	0.0030
$10 < D < 20$ km	44	0.0479	0.0039
$6 < D < 10$ km	126	0.0473	0.0066
$4 < D < 6$ km	183	0.0481	0.0082
$2 < D < 4$ km	507	0.0495	0.0097
Population	# of objects	Median $\sin(i)$	Std( $\sin(i)$ )
All	2037	0.0367	0.0017
$D > 20$ km	10	0.0369	0.0008
$10 < D < 20$ km	44	0.0369	0.0016
$6 < D < 10$ km	126	0.0371	0.0014
$4 < D < 6$ km	183	0.0370	0.0020
$2 < D < 4$ km	507	0.0367	0.0019

Figure 2: An  $(a, e)$  (panel A) and  $(a, \sin(i))$  (panel B) projection of the HCM (black dots) and SDSS (blue circles) Koronis family members. Vertical red lines display the location of the main mean-motion resonances in the region.

the local dynamics), and, following the approach of Carruba and Nesvorný (2015c) objects with  $2 < D < 4$  km ( $D_3$  population hereafter; the sizes of asteroids without WISE data information where computed using the mean value of the geometric albedo for the Koronis family from Nesvorný et al. (2015) and Eq. 1 in Carruba et al. (2003)). Panel B shows a similar histogram, but for the distribution in proper  $\sin(i)$ . Table 1 reports the values of mean and standard deviation for the different size populations of the 2037 Koronis sample (about 40% of the original family) in proper  $e$  and  $\sin(i)$ . At smaller sizes the spread in  $\sin(i)$  increases, but this essentially stops at sizes lower than 4 km in diameter.

Rather than being a real characteristics of the Koronis family, we believe that this is an artifact caused by the method used to identify the family in proper element domain. As discussed in Brož and Morbidelli (2013) and Carruba et al. (2013), the hierarchical clustering method (HCM) may fail to identify the periphery, or halo, of some large families such as Eos and Koronis. To overcome this limitation, we used the SLOAN and WISE data to identify objects in the vicinity of the HCM Koronis family with a S-complex taxonomy. The Koronis family is special among asteroid families since it is a S-type family surrounded by a population of C-type objects. We selected objects whose semi-major axis is between the centers of the 5J:-2A and 7J:-3A mean-motion resonances, whose  $e$  is between 0 and 0.115 (minimum and maximum values of  $e$  of

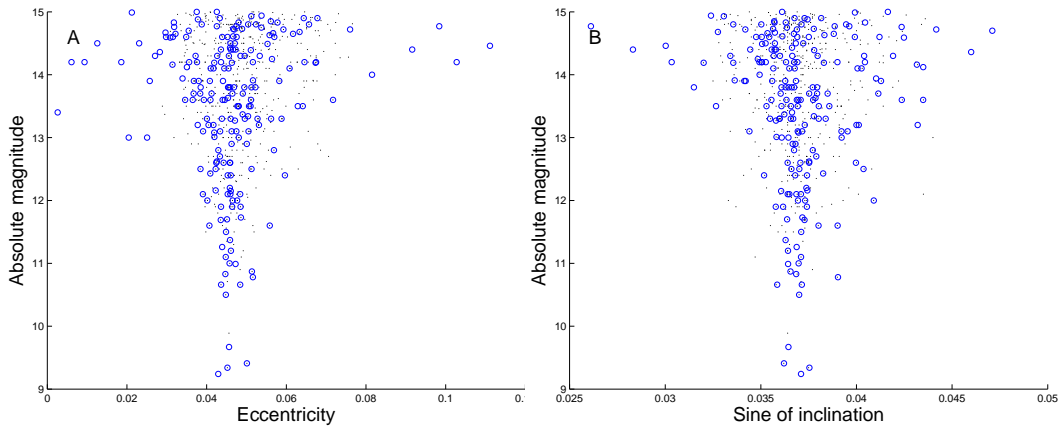


Figure 3: An  $(e, H)$  (panel A) and  $(\sin(i), H)$  (panel B) projections of members of the HCM (black dots) and SDSS (blue circles) Koronis family. The SDSS and, slightly so, the HCM families have a characteristic V-shape structure in these domains.

Koronis members  $\pm 0.015$ , Nesvorný et al. (2015), and  $\sin(i)$  is between 0.000 and 0.085 ( $\pm 0.04$  from maximum and minimum family range). After eliminating objects with taxonomies in the C-complex, whose value of  $p_V$  is less than 0.1, and whose values of  $e$  and  $\sin(i)$  differ from the center of the family by more than 4 standard deviations of the distribution (see Carruba and Nesvorný (2015c) for more detail on the rationale on the use of these criteria, using a  $3\sigma$  criteria produces changes in the family membership of less than 1%, a  $5\sigma$  criteria includes in the Koronis family too many C-type objects), we obtained a total sample of 612 asteroids that could potentially be members of the extended SDSS Koronis family, of which 467 are members of the HCM Koronis core, as identified in Nesvorný et al. (2015), and 145 are in the family halo. While the number of SDSS objects is inferior to that of the dynamical HCM Koronis family, and complete only for values of  $H$  greater than 13.5 (DeMeo and Carry, 2013), we believe that the possibility of identifying a wider population in  $e$  and  $\sin(i)$  far outweighs the limitation in completeness of the Koronis SDSS sample.

Table 2: Number of objects, median, and standard deviation for the different size populations of the 238 Koronis SDSS sample in proper  $e$  and  $\sin(i)$ .

Population	# of objects	Median $e$	Std( $e$ )
All	232	0.0469	0.0148
$D > 20$ km	9	0.0468	0.0032
$10 < D < 20$ km	19	0.0462	0.0036
$6 < D < 10$ km	37	0.0449	0.0070
$4 < D < 6$ km	59	0.0438	0.0112
$2 < D < 4$ km	108	0.0439	0.0190
Population	# of objects	Median $\sin(i)$	Std( $\sin(i)$ )
All	232	0.0370	0.0027
$D > 20$ km	9	0.0370	0.0009
$10 < D < 20$ km	19	0.0372	0.0011
$6 < D < 10$ km	37	0.0372	0.0012
$4 < D < 6$ km	59	0.0373	0.0024
$2 < D < 4$ km	108	0.0368	0.0033

Fig. 2 displays the  $(a, e)$  (panel A) and  $(a, \sin(i))$  (panel B) projections of the HCM (black dots) and SDSS Koronis family (blue circles). As discussed in Cellino et al. (2004, 2009), and

shown in Fig. 3 the SDSS Koronis family displays a V-shape distribution in the  $(e, H)$  and  $(\sin(i), H)$  plane, where  $H$  is the asteroid absolute magnitude. Table 2 displays values of mean and standard deviation for the different size populations of the halo Koronis sample in proper  $e$  and  $\sin(i)$ , that are also shown in Fig. 4, just for size bins with a population of asteroids larger than 30, so as to have a statistical significant sample. If we assume that errors on the standard deviations in proper  $e$  and  $\sin(i)$  are proportional to  $\sqrt{(n)}/n$ , with  $n$  the number of objects in each size bin, then that would correspond to rejecting samples with a error larger than  $\simeq 20\%$ . By using this approach we are consistent with the method of other authors ((Masiero et al., 2011)), that also did not considered populations of asteroids with  $D > 12$  km to avoid small-number statistics issues. For the sake of brevity, we will define the  $6 < D < 10$ ,  $4 < D < 6$ , and  $2 < D < 4$  km size bins as  $D_8$ ,  $D_5$ , and  $D_3$  populations, respectively. We eliminated asteroids with proper  $a > 2.88$  AU to avoid including objects that crossed the  $g + 2g_5 - 3g_6$  secular resonance and other local mean-motion resonances. To estimate the contribution of background objects to the SDSS Koronis family, following the approach of Brož and Morbidelli (2013) we counted the number of S-complex objects in boxes in the  $(a, e)$  and  $(a, \sin(i))$  planes, limited in  $a$  by the 5J:-2A mean-motion resonance and  $a < 2.88$  AU, and in  $e$  and  $\sin(i)$  by the center of the distribution plus  $4 \sigma$  values of the real family as the minimum value, and this quantity plus the length of the distribution in  $e$  and  $\sin(i)$  of the real family as the maximum value. The maximum number of S-complex objects that we found in these boxes was 6 objects, which corresponds to 2.1% of the population of the Koronis SDSS family in that area (238 asteroids). Overall, this seems to suggest that our determination of the Koronis family halo should not be too much affected by background contributions. Also, possible errors caused by the (maximum) 5% photometric noise in the SDSS-MOC4 data used in the DeMeo and Carry (2013) taxonomic identification method should affect at most 1% of the SDSS Koronis family S-complex objects, according to our estimates.

Distributions in  $e$  and  $\sin(i)$  became more spread at smaller sizes, and in a steeper way with respect to what found for the nominal HCM core of the Koronis family. The dependence of  $\sigma(e)$  and  $\sigma(\sin(i))$  with respect to  $D$  is similar. Assuming that  $\sigma$  follows a power-law of the form  $\sigma = C(\frac{1}{D})^\alpha$ , best-fit values of  $\alpha$  for size bins with more than 30 objects, red line in Fig. 4, are 1.02 and 0.95 for the  $e$  and  $\sin(i)$  distributions, with characteristic errors of approximately 9% and 3%, respectively. Both distributions seem to be inversely proportional with respect to asteroid diameters (i.e.,  $\sigma = C\frac{1}{D}$ ).

### 3. Local dynamics

To better understand the importance of the local web of mean-motion and secular resonances, we obtained dynamical maps in the domain of synthetic proper  $(a, e)$  and  $(a, \sin(i))$  with the method of Carruba (2010). Dynamical maps do not account for non-conservative forces such as the Yarkovsky force, but are useful to identify the location of the main mean-motion and secular resonances in proper element domains. We used 1775 particles in the osculating  $(a, e)$  plane, using a step of 0.002 AU in  $a$  and 0.005 in  $e$ , with 71 intervals in  $a$  and 25 in  $e$  starting at  $a = 2.82$  AU and  $e = 0$ , respectively. In the osculating  $(a, \sin(i))$  plane we used the same intervals in  $a$ , and 51 intervals of  $0.06^\circ$  in osculating  $i$ , starting at  $i = 0^\circ$ , for a total of 3621 particles. Test particles were integrated over 20 Myr under the influence of all planets, except Mercury (whose presence was accounted for as a barycentric correction to the mass of the Sun), with a time step of 20 days.

Fig. 5 shows our results in the proper  $(a, e)$  (panel A) and proper  $(a, \sin(i))$  (panel B) plane. Mean-motion resonances appear as vertical strips devoid of particles, secular resonances cause

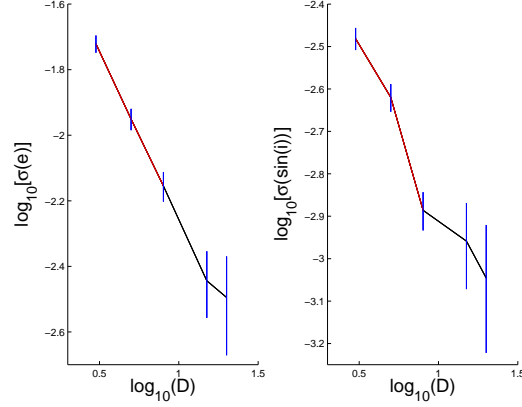


Figure 4: Log-log plots of the dependence of the standard deviation of the distribution in  $e$  and  $\sin(i)$  of the Koronis halo members, as a function of diameter. Vertical blue lines display the nominal errors, assumed to be inversely proportional to the square root of the number of objects in each size bin. The red line connects size bins with more than 30 objects and nominal errors less than 5%.

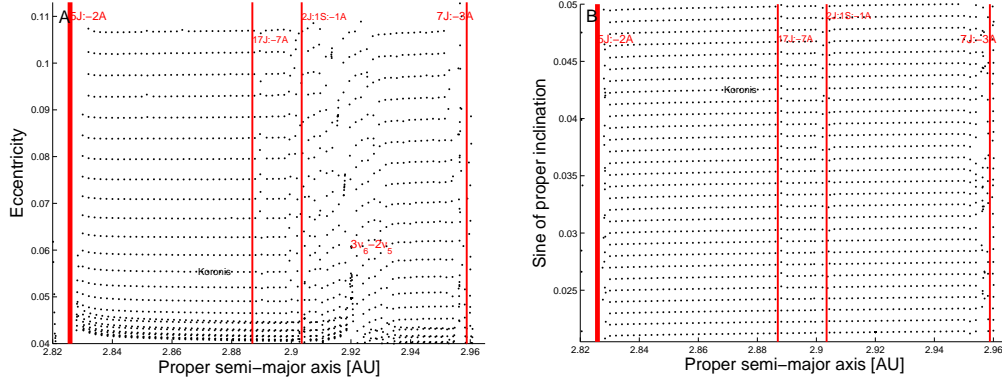


Figure 5: A dynamical map in the domain of proper  $(a, e)$  (panel A) and proper  $(a, \sin(i))$  (panel B) for the region of the Koronis family. Black dots display the location in the two proper elements domains of each test particle that survived for the length of the integration. Vertical red lines display the location of the local mean-motion resonances.

particles to be aligned in inclined bands. Apart from the well-know 5J:-2A and 7J:-3A mean-motion resonances, we also identified the 17:-7A two-body resonance and the 2J:1S:-1A three-body resonance in the region (a minor role is also played by the 6S:-1A two body resonance with Saturn, near the 2J:1S:-1A three-body resonance). No major secular resonances appear in the  $(a, \sin(i))$  plane. In the  $(a, e)$  plane, however, one can notice the strong effect of the  $3\nu_6 - 2\nu_5$  secular resonance, that appears as an inclined band at  $\simeq 2.92$  AU.

To check if all important secular resonances were identified in the dynamical maps, we also computed the orbital location of all secular resonances whose combination of proper  $g$  and  $s$  is within the values covered by the Koronis family, and checked the number of likely resonators (Carruba, 2009) for each resonance (likely resonators are defined as the objects whose combination of asteroidal proper frequencies is within  $\pm 0.3$  arcsec/yr from the resonance center. For the case of the  $z_1 = g - g_6 + s - s_6$  resonance, this would correspond to  $g + s = g_6 + s_6 = 1.898$  arcsec/yr; the actual threshold may vary for higher order resonances, but the 0.3 arcsec/yr boundary usually provide a good first order of magnitude criteria). Not all likely resonators are in librating states, but the number of these objects may provide a first clue on the dynamical strength of each resonance.

Table 3: Main secular resonances in the Koronis region, frequency value, and number of likely and actually resonant asteroids.

Resonance argument	Frequency value ["/yr]	Likely resonators
g resonances		
$g - 3g_6 + 2g_5$	76.215	167
s resonances		
$s - s_6 + 2g_6 - 2g_5$	-74.317	42

Table 3 shows the results for the two secular resonances with a number of likely resonators larger than 1: the  $3\nu_6 - 2\nu_5 = g - 3g_6 + 2g_5$  resonance, already described in the seminal paper of Bottke et al. (2001), and the  $2\nu_5 - 2\nu_6 + \nu_{16} = s - s_6 + 2g_6 - 2g_5$   $s$ -type resonance, that is near the 7J:-3A mean-motion resonance and has therefore a limited importance in affecting the dynamical evolution of the Koronis group. The very limited number of secular resonances with a significant population of likely resonators found in this region confirms our initial hypothesis that the Koronis family lies in a relatively dynamically quiet region.

How much the local dynamics can be responsible for the current dispersion in proper  $e$  and  $\sin(i)$  of the Koronis family? To answer this question, we performed simulations with the *SYSYCE* integrator (Swift+Yarkovsky+Stochastic YORP+Close encounters) of Carruba et al. (2015a), modified to also account for past changes in the values of the solar luminosity. The numerical set-up of our simulations was similar to what was discussed in Carruba et al. (2015a): we used the optimal values of the Yarkovsky parameters discussed in Brož et al. (2013) for S-type asteroids (the spectral type of most Koronis family members), the initial spin obliquity was random, and normal reorientation timescales due to possible collisions as described in Brož (1999) were considered for all runs. We warn the reader that using other values of key parameters, such as the bulk density and thermal conductivity of asteroids may significantly alter the strength of the Yarkovsky force (Masiero et al., 2012). For a review of the effect of changing these parameters on the estimated age of the Koronis family please see Carruba et al. (2015b). We integrated our test particles under the influence of all planets, and obtained synthetic proper elements with the approach described in Carruba (2010). Initial conditions for the 502 test particles for the Koronis family were obtained with the approach described in Carruba et al. (2015b), i.e, we generated a fictitious family with the ejection parameter  $V_{EJ}$  equal to that obtained from our

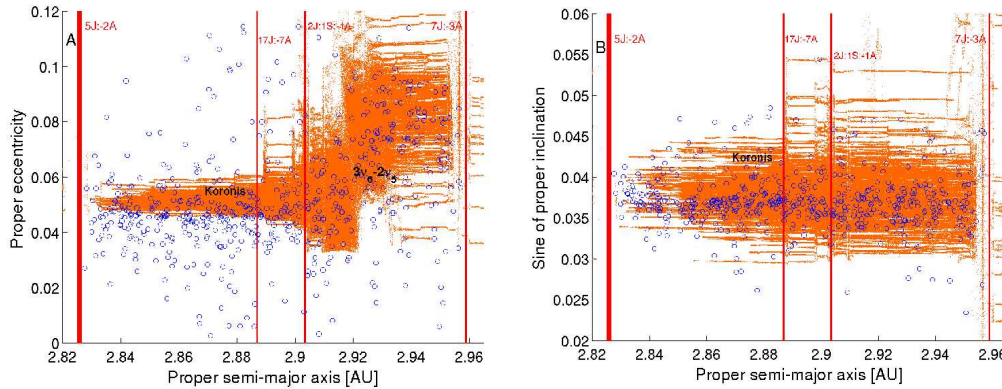


Figure 6: Dynamical evolution of test particles (dark orange dots) in the proper  $(a, e)$  (panel A) and proper  $(a, \sin(i))$  (panel B) planes for the Koronis family. Blue circles identify the orbital location of SDSS members, the other symbols are the same as in Fig. 2.

Monte Carlo simulations of the Koronis family, i.e., 60 m/s. The size distribution of the test particles used followed a size-frequency distributions (SFD) with an exponent  $-\alpha$  that best-fitted the cumulative distribution equal to 3.6, a fairly typical value (Masiero et al., 2012), and with diameters in the range from 2.0 to 12.0 km.

Fig. 6 displays the dynamical evolution of our test particles in the proper  $(a, e)$  (panel A) and proper  $(a, \sin(i))$  (panel B) planes (each orange path represent values of proper element for each given particle). Blue circles identify the orbital location of SDSS Koronis members, vertical red lines display the location of mean-motion resonances. As in Bottke et al. (2001) we observe the very relevant effect of the  $3\nu_6 - 2\nu_5$  secular resonance in increasing values of proper eccentricities. We were not able, however, to produce the low-eccentricity population of asteroids at  $a < 2.88$  au. This may be caused by either i) the fact that the family identified in SDSS data may be too extended in eccentricity, ii) some other mechanism of dynamical mobility in proper  $e$  not accounted in our model, such as close encounters with massive asteroids and dwarf planets (Carruba et al., 2003) or pericenter secular resonances with Ceres (Novaković et al., 2015) could have been at play, or iii) that our simulations did not account in a large enough manner for reorientations events of particles across mean-motion and secular resonances that may have caused further spread in eccentricity (see also the discussion in the next section). Since the goal of this paper was to concentrate on the inclination distribution of the Koronis family, we believe this is an acceptable trade-off. But explaining the current distribution in proper  $e$  of the Koronis family certainly remain a challenge for future research. A few particles interacted with the  $2\nu_5 - 2\nu_6 + \nu_{16}$  nodal resonance near the 7J:-3A mean-motion resonance and were scattered to higher values of inclination, as a result.

To compute how much local dynamics influenced the dispersion in proper  $e$  and  $\sin(i)$ , we calculated the time behavior of the standard deviation of  $\delta(e)$  and  $\delta[\sin(i)]$  for all 502 particles. Standard deviations of changes in  $e$  and  $\sin(i)$  with respect to their initial values were computed so as to eliminate the effect of the assumed initial dispersion and obtain an estimate of changes caused by dynamics. We did not consider in our computation particles that escaped from the region of the Koronis family, defined as a box given by the current maximum and minimum values in  $(a, e, \sin(i))$ .

Fig. 7 displays our results, for particles in the size range from 4 to 6 km, while Table 4 summarizes different values for three size interval distributions ( $D_8, D_5$ , and  $D_3$  populations).

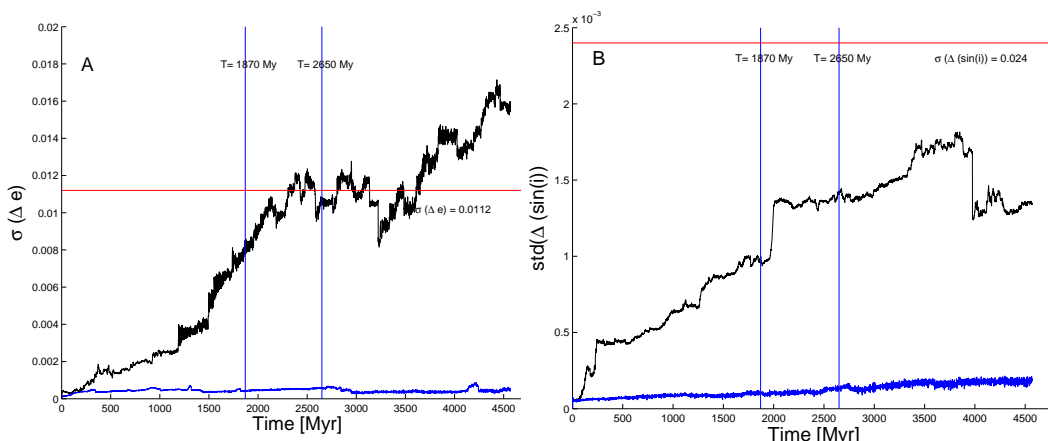


Figure 7: Temporal evolution of the standard deviations in proper  $\delta(e)$  (panel A) and  $\delta[\sin(i)]$  (panel B) for the particles in the size range from 4 to 6 km ( $D_5$ ) in our simulation. The black line refers to the whole Koronis sample, while the blue line is just for the  $a < 2.88$  au population. Vertical lines display the minimum and maximum ages of the family, as estimated in Carruba et al. (2015b) using a Yarko-YORP method to fit the distribution in proper semi-major axis. The horizontal red line displays the current value of dispersion in proper  $e$  and  $\sin(i)$  for the  $a < 2.88$  au population, as from Table. 2.

Changes in  $\delta(e)$  and  $\delta[\sin(i)]$  in the region with  $a < 2.88$  au are small, and amount at most to just 5% of the currently observed values of standard deviations in  $\delta(e)$  and  $\delta[\sin(i)]$ . If we consider the whole Koronis family, however, changes in  $\delta(e)$  are of the order of 93%, and in  $\delta[\sin(i)]$  of 50% for the Koronis SDSS sample with  $4 < D < 6$  km, respectively. Overall, these results suggest that a significant part of the spread in proper  $\sin(i)$  (and less so for proper  $e$ ) for the  $a < 2.88$  au Koronis population could still bear traces of the original ejection speeds <sup>2</sup>.

This could also explain the dependence of standard deviations in  $e$  and  $\sin(i)$  as a function of the asteroid diameter, found in Sect. 2. Two values of speed can be computed for the fragments of a collision. One defines the ejection speeds of the objects immediately after the collision. The second one characterizes the speed after the fragments escape the gravitational pull of the parent body, or velocity at infinity. In this work we will define the first speed as initial ejection speed, and the latter as terminal ejection speed, so as to avoid the cumbersome expression “ejection speed at infinity”. If one assumes that the initial ejection velocity field follows a Gaussian distribution of zero mean and standard deviation given by (Vokrouhlický et al., 2006):

$$\sigma_{V_{ej}} = V_{EJ} \cdot \frac{5km}{D}, \quad (1)$$

<sup>2</sup>To check how robust and model-independent are our results, we compared the time evolutions the standard deviation of changes in proper  $e$  and  $\sin(i)$  obtained by our integration with those obtained by Bottke et al. (2001) in their seminal work on the Yarkovsky effect and the Koronis family. In their model there were no reorientations, all particles had 4 km diameters, spin axes were randomly distributed and fixed, and the integration lasted  $\simeq 600$  Myr, under the influence of all planets. Despite the differences in which non-gravitational forces were modeled, we found that i) changes in standard deviation of  $\delta e$  and  $\delta[\sin(i)]$  were essentially negligible in the  $a < 2.88$  au region of the Koronis family, as observed in our simulations (blue lines in Fig. 7), and ii) differences for the whole Koronis family were at most of the order of 20%. Since standard deviations in  $\delta e$  and  $\delta[\sin(i)]$  produced by dynamics sum quadratically with those from the current observed distribution (see Eq. 5), a 20% difference corresponds to a 4% error, which is acceptable, in our opinion.

Table 4: Standard deviations of changes in proper  $e$  and  $\sin(i)$  at the minimum and maximum age estimate for the Koronis family, for three size distributions of the simulated dynamical group for the whole family and for  $a < 2.88$  au population.

Size int. [km]	Min $\sigma[\delta(e)]$	Max $\sigma[\delta(e)]$	Min $\sigma[\delta(\sin(i))]$	Max $\sigma[\delta(\sin(i))]$
Whole sample				
$D_8$	0.0051	0.0063	0.0006	0.0009
$D_5$	0.0085	0.0104	0.0010	0.0014
$D_3$	0.0099	0.0169	0.0015	0.0021
$a < 2.88$ au pop.				
$D_8$	0.0002	0.0003	0.0001	0.0001
$D_5$	0.0004	0.0006	0.0001	0.0001
$D_3$	0.0006	0.0008	0.0001	0.0002

where  $D$  is the body diameter in km, and  $V_{EJ}$  is a parameter describing the width of the initial velocity field, then the dependence of  $\sigma_{V_{Ej}}$  on  $D$  should be inverse. Carruba and Nesvorný (2015c) described how ejection speeds are related to distributions in proper  $e$  and  $\sin(i)$ . If, as suggested by the results of our simulations, the current distribution in  $e$  and  $i$  of the Koronis family should have been less affected by dynamics than those of proper  $a$ , at least for  $a < 2.88$  au, then one would expect that, to some limits, the dependence of  $\sigma_e$  and  $\sigma_{\sin(i)}$  on  $D$  should still be roughly inverse, as observed. We will further investigate this issue in the next section.

#### 4. Ejection velocity field

Proper orbital elements can be related to the components of terminal ejection velocity along the direction of orbital motion ( $\delta v_t$ ), in the radial direction ( $\delta v_r$ ), and perpendicular to the orbital plane ( $\delta v_W$ ) through the Gauss equations (Murray and Dermott, 1999):

$$\frac{\delta a}{a} = \frac{2}{na(1-e^2)^{1/2}}[(1 + \cos(f))\delta v_t + (e \sin(f))\delta v_r], \quad (2)$$

$$\delta e = \frac{(1-e^2)^{1/2}}{na} \left[ \frac{e + \cos(f) + e \cos^2(f)}{1 + \cos(f)} \delta v_t + \sin(f) \delta v_r \right], \quad (3)$$

$$\delta i = \frac{(1-e^2)^{1/2}}{na} \frac{\cos(\omega + f)}{1 + \cos(f)} \delta v_W. \quad (4)$$

where  $\delta a = a - a_{ref}$ ,  $\delta e = e - e_{ref}$ ,  $\delta i = i - i_{ref}$ , where  $a_{ref}$ ,  $e_{ref}$ ,  $i_{ref}$  define a reference orbit and  $f$  and  $\omega$  are the true anomaly and perihelion argument of the disrupted body at the time of impact. Since proper  $a$  is affected by non-gravitational forces such as the Yarkovsky and YORP effects, it is not therefore possible to use the first equation to obtain information on the primordial values of the components of the terminal velocities. In this section we focus our attention on the proper  $e$  and  $i$  distribution, for  $a < 2.88$  au.

Concerning values of  $e_{ref}$  and  $i_{ref}$ , since the Koronis family originated from a catastrophic disruption event that left no main largest fragment (Nesvorný et al., 2015), we obtained an estimate of the barycenter position in the  $(a, e, \sin(i))$  domain. Apart for the few asteroids for which a mass determination was available in Carry (2012), we estimated the masses of the other objects using the WISE values of diameters and the density of 243 Ida, the only member of Koronis visited by the space mission Galileo, as reported in Carry (2012). Values of  $a_b$ ,  $e_b$ ,  $\sin(i_b)$  at the barycenter were then obtained by means of a weighted average, with the weight on the asteroid proper elements given by each asteroid estimated mass, divided by the total mass of the family. We first analyzed how the current  $e$  distribution of the  $a < 2.88$  au population depends

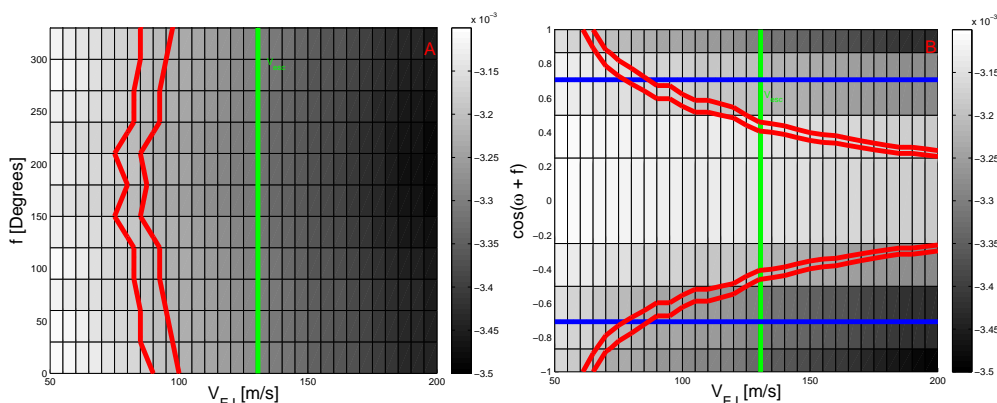


Figure 8: Values of  $\sigma_{\sin(i)}$  as a function of  $f$  and  $V_{EJ}$  (panel A) and  $\cos(\omega + f)$  and  $V_{EJ}$  (panel B). Red lines display the range of value observed for the current  $D_3$  population, from 0.0031 to 0.0035. The vertical green lines display the value of minimum estimated escape velocity from the Koronis parent body. The horizontal blue lines in panel B show values of  $\cos(\omega + f) = \frac{\sqrt{2}}{2}$ .

on  $f$ . For this purpose, we generated a grid of 31 by 13 fictitious Koronis families with values of  $V_{EJ}$ , the parameter determining the spread of the initial ejection velocity field (see Eq. 5 in Carruba and Nesvorný (2015c), going from 50 to 200 m/s, and  $f$  from 0 to  $360^\circ$ . We then computed the standard deviation of these fictitious families, and compared their values with the current one for the  $D_3$  population (0.0190), with an assumed 5% error (at this stage of our analysis, we neglected the effect of dynamical evolution in proper  $e$ , see Fig. 11 for a qualitative understanding of the dependence of  $\sigma_e$  on  $V_{EJ}$  and  $f$ ). The minimum possible value of  $V_{EJ}$  is 170 m/s, which is quite higher than the estimated escape velocity from the Koronis parent body (130.6 m/s, assuming that the diameter of the parent body was 122 km, the minimum value in the literature, Nesvorný et al. (2015)). This may suggest that the current distribution in proper  $e$  of the  $a < 2.88$  au population might be significantly affected by dynamical evolution. The situation is different for the  $a < 2.88$  au  $\sin(i)$ . Again, we generated fictitious Koronis families with different values of  $f$  and  $(f + \omega)$ , and of  $V_{EJ}$ , compute their standard deviation, and compared with the current one for the  $D_3$  population (0.0033), with an assumed 5% error. Fig. 8 displays our results in the  $(V_{EJ}, f)$  (panel A) and  $(V_{EJ}, \cos(\omega + f))$  (panel B) planes. The vertical green line displays the estimated escape velocity from the Koronis parent body. In the first case we assumed that  $(\omega + f) = 45^\circ$ , while in the second we used  $f = 180^\circ$ .

Our results show that the  $\sin(i)$  distribution does not depend significantly on  $f$ , as expected from the analysis of the denominator of Eq. 4, and the fact that the mean eccentricity of Koronis members is small (of the order of 0.05). Essentially values of  $V_{EJ}$  in a strip from 75 to 100 m/s would all produce families consistent with the current distribution in  $\sin(i)$  regardless of the original value of  $f$ . The situation is different for  $\omega + f$ . Using  $f = 180^\circ$ , the value of  $f$  that provided the best results in the previous analysis (all values of  $f$  are of course admissible, according to Eq. 4, here we just picked the one that provided the most optimal result in our previous analysis), we obtain values of the standard deviation in  $\sin(i)$  as a function of  $V_{EJ}$  and  $\omega + f$  (Fig. 8, panel B). The minimum value of  $\cos(\omega + f)V_{EJ}$  is of the order of 60 m/s. If one assumes that  $V_{EJ}$  does not much exceed the escape velocity, since this would imply very energetic impacts, which are quite rare (Bottke et al., 2015), then values of  $\cos(\omega + f)$  in the range from -0.2 to 0.2 can be excluded. According to this analysis, values of  $\omega + f$  from  $78.5^\circ$  to  $101.5^\circ$  (and the analogous negative range) should therefore be unlikely.

What values of the  $V_{EJ}$  parameter would we expect for the initial ejection velocity field of

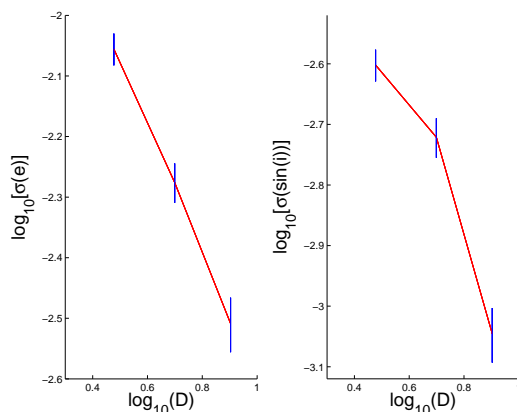


Figure 9: Log-log plots of the dependence of the standard deviation of the distribution in  $e$  and  $\sin(i)$  of the Koronis SDDS family members, as a function of diameter, when corrections caused by the dynamical evolution are accounted for. Vertical blue lines display the nominal errors, assumed to be inversely proportional to the square root of the number of objects in each size-bin.

the Koronis family, before dynamical effects occurred? In Sect.3 we computed changes in  $\sin(i)$  for simulated members of the Koronis family, for three different size ranges. If we assume that changes in  $\sin(i)$  caused by dynamical processes and by the initial velocity distribution can be summed as two independent random variables, which should be the case for families, such as Koronis, not affected by powerful secular resonances such as the  $nu_6$ ,  $z_1$  or  $z_2$  resonances, then the initial standard deviation of  $\sin(i)$  associated with the original ejection velocity field,  $\sigma_{\sin(i)}$ , can be obtained from the relationship:

$$\sigma_{\sin(i)} = \sqrt{\sigma_{cur}^2 - \sigma_{dyn}^2}, \quad (5)$$

where  $\sigma_{cur}$  is standard deviation of the current distribution of either  $e$  or  $\sin(i)$  values, and  $\sigma_{dyn}$  is the standard deviation of changes caused by dynamics. We computed the standard deviations of  $e$  and  $\sin(i)$  corrected for the effects of dynamical evolution using Eq. 5 and data from Table 4, as a function of asteroid diameters. If we use the data on the diffusion caused in the area with  $a < 2.88$  au, the distributions still follow a power-law of the form  $\sigma = C(\frac{1}{D})^\alpha$ , with  $\alpha = 1.02$  and  $0.95$ , with the same errors discussed in Sect 2. To within a 9% error, this law is compatible with an inverse relationship of the form  $\sigma = C(\frac{1}{D})$ , that also applies to  $v_W$  through Eq. 4. If we use data on the dispersion computed for the whole family, and obtain  $\sigma_{cur}$  using Eq. 5, then the values of  $\sigma_{cur}$ , shown in Fig. 9, are lower. However,  $\alpha = 1.06 \pm 0.14$  and  $1.03 \pm 0.13$  are still compatible with an inverse relationship.

Assuming that that is true, what value of  $V_{EJ}$  in Eq. 1 could best describe the initial spread in  $\sin(i)$  (and possibly  $e$ )? We created various fictitious families for the three Koronis size intervals in  $D$  previously studied ( $6 < D < 10$ ,  $4 < D < 6$ ,  $2 < D < 4$  km), and two values of the diameter of the Koronis parent body, one obtained extrapolating the current observed SFD down to zero km ( $D_{PB}=122$  km), and the second by using Durda et al. (2007) approach ( $D_{PB}=180$  km, see also Nesvorný et al. (2015)). Since the SFD's of old families are usually depleted by collisional and dynamical evolution, Durda et al. (2007) approach that use only bodies with  $D > 10$  km is often preferred. We assume that the initial ejection speeds were isotropic, and we used different values of  $\cos(\omega + f)$  in the range from -1 to 1, and  $V_{EJ}$  from 40 to 200 m/s. We did not sample the interval of  $\cos(\omega + f)$  between -0.2 and 0.2, since this was excluded by our previous analysis.

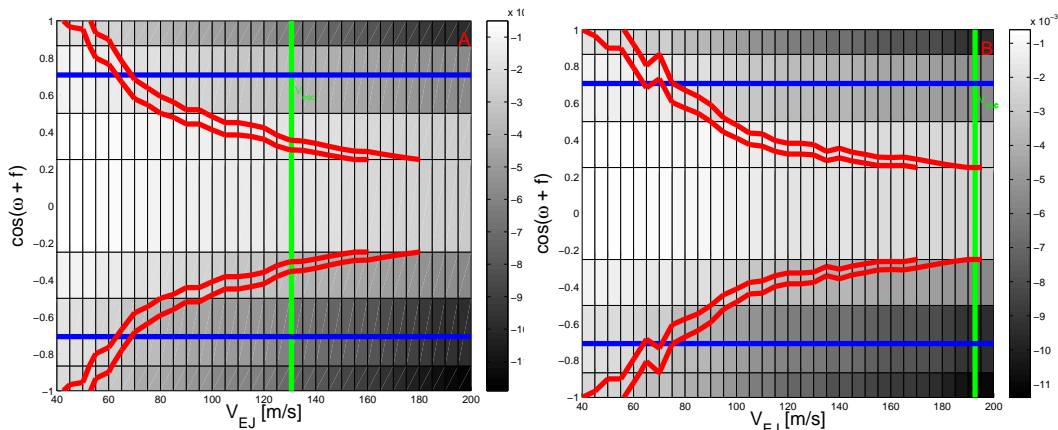


Figure 10: Values of the standard deviation in  $\sin(i)$  of simulated Koronis family  $D_3$  populations and  $D_{PB} = 122$  km (Panel A), and  $D_{PB} = 180$  km (Panel B). The vertical green lines display the values of escape velocity, while blue lines are associated with  $\omega + f = 45^\circ$ . The red lines have the same meaning as in Fig. 8.

For the values of the current spread, we used those corrected for the effects of the whole Koronis family dynamics.

Our results for the  $D_3$  population are displayed in Fig. 10 (for the sake of brevity, we do not show the results for the  $D_5$  and  $D_8$  size populations). With the assumption of isotropic initial speeds, minimum values of  $V_{EJ}$  are in the range from 40 to 55 m/s. Distributions are in good agreement, and compatible with what obtained by Yarko-Yorp methods for the distribution in proper  $a$  (70 m/s, Carruba et al. 2015b).

Finally, Fig. 11 shows a contour plot of standard deviations in eccentricity for simulated Koronis family  $D_3$  population, with  $D_{PB} = 122$  km (for the sake of brevity, we do not show the results for  $D_{PB} = 180$ ). If we account for the effects of dynamics on the whole Koronis family, the new minimum value of  $V_{EJ}$ , 80 m/s is now lower than the minimum escape velocity from Koronis parent body, and in agreement with results from the  $\sin(i)$  distribution, assuming that  $-0.6 < \cos(\omega + f) < 0.6$ .

The large correction from dynamical effects, not observed for the  $a < 2.88$  au population, may be caused by the fact that our Koronis simulated sample was limited (502 particles) and/or not able to fully reproduce the effect of particles reorienting their spin axis and inverting the direction of migration from higher to lower  $a$ . Perhaps this may suggest that the stochastic YORP effect may not be that “stochastic”, meaning that longer timescales for choosing new asteroid shape models (and consequently, more reorientation events) could be closer to what happens in nature. A static YORP effect is actually needed to explain the ecliptic latitude distribution of main belt asteroids (Hanuš et al., 2013) or the Slivan states of some Koronis family members (Vokrouhlický et al., 2003). Alternatively, if we only consider the results of our dynamical simulation for the  $a < 2.88$  au population, the initial ejection velocity field could have been rather unisotropic, with lower values of  $\delta v_W$  and larger values of  $\delta v_r$  and  $\delta v_t$ . Further study is needed to clarify this issue.

## 5. Conclusions

The main results of this work can be summarized as follows:

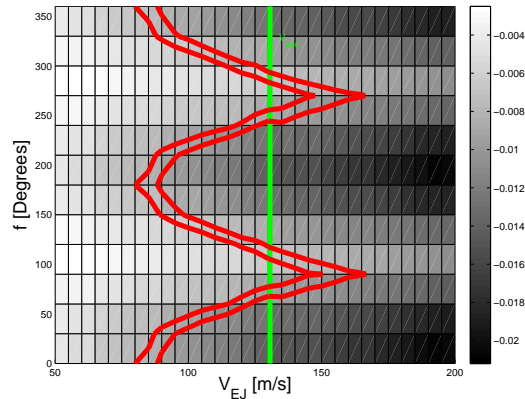


Figure 11: Values of the standard deviation in  $e$  of simulated Koronis family  $D_3$  populations and  $D_{PB} = 122$  km. Red and green lines have the same meaning as in Fig. 10.

- We identified the Koronis family in the domain of proper elements and used SDSS-MOC4 and WISE data to identify members of the Koronis halo, so as to obtain better estimates of the current spread in proper  $e$  and  $\sin(i)$  of the family. It has been assumed that the spread of the original ejection velocity field (and therefore of  $e$  and  $\sin(i)$ , Carruba and Nesvorný (2015c)) should actually be inversely proportional to  $D$  (Vokrouhlický et al., 2006). Here we show that this is actually the case for the Koronis family.
- We studied how the local dynamics may have affected the original distribution in proper  $e$  and  $\sin(i)$  of the Koronis family by obtaining dynamical maps of the Koronis orbital region, and by performing numerical integrations of a fictitious family with the *SYSYCE* integrator of Carruba et al. (2015a). Local dynamics for the whole family affects more eccentricities than inclination: about all of the current spread in eccentricity could be caused by dynamical effects. Conversely, up to 50% of the current spread in inclination can be original.
- We estimated the original dispersion of the Koronis family in proper eccentricity and inclination, assuming that changes caused by dynamical processes and by the initial velocity distribution can be summed as two independent random variables. Estimated values of the  $V_{EJ}$  parameter describing the initial spread of the Koronis family should be of the order of 80 m/s, and compatible with what previously found with Yarko-YORP methods to fit the Koronis family semi-major axis distribution (70 m/s).

Overall, for the first time we obtained estimates of the  $V_{EJ}$  parameter describing the initial spread of the Koronis family using the *inclination* distribution, rather than the semi-major axis one, as previously attempted. Our results suggests that i) the initial spread in ejection velocity might indeed be inversely dependent on the asteroid sizes, as previously assumed by other authors (Vokrouhlický et al., 2006), and ii) values of  $V_{EJ}$  could be compatible with what previously obtained by using Yarko-Yorp methods to fit the semi-major axis distribution of the Koronis family. Extending this analysis to other families identified in Carruba and Nesvorný (2015c) as good candidates for not being too much affected by dynamical evolution, remains a challenge for possible future research.

## Acknowledgments

We are grateful to the reviewers of this paper, Drs. Bojan Novaković and Miroslav Brož, for comments and suggestions that greatly improved the quality of this work. We thank Dr. William F. Bottke for allowing us to use the results of his dynamical simulation of the Koronis family from the Bottke et al. (2001) paper. This paper was written while the first author was a visiting scientist at the Southwest Research Institute (SWRI) in Boulder, CO, USA. We would like to thank the São Paulo State Science Foundation (FAPESP) that supported this work via the grants 14/24071-7 and 13/15357-1. D.N.'s work on this project was supported by NASA's Solar System Workings program. This publication makes use of data products from the Wide-field Infrared Survey Explorer, which is a joint project of the University of California, Los Angeles, and the Jet Propulsion Laboratory/California Institute of Technology, funded by the National Aeronautics and Space Administration. This publication also makes use of data products from NEOWISE, which is a project of the Jet Propulsion Laboratory/California Institute of Technology, funded by the Planetary Science Division of the National Aeronautics and Space Administration.

## References

- Bendjoya, P., Zappalà, V. 2002. Asteroid Family Identification. Asteroids III, W. F. Bottke Jr., A. Cellino, P. Paolicchi, and R. P. Binzel (eds), University of Arizona Press, Tucson, 613-618.
- Binzel, R. P., Xu, S., Bus, S. J. 1993. Spectral variations within the Koronis family - Possible implications for the surface colors of Asteroid 243 Ida. *Icarus* 106, 608.
- Bottke, W. F., Vokrouhlický, D., Brož, M., Nesvorný, D., Morbidelli, A. 2001. Dynamical Spreading of Asteroid Families by the Yarkovsky Effect. *Science* 294, 1693-1696.
- Bottke, W. F., Vokrouhlický, D., Walsh, K. J., Delbó, M., Michel, P., Lauretta, D. S., Campins, H., Connolly, H. C., Scheeres, D. J., Chelsey, S. R. 2015. In search of the source of asteroid (101955) Bennu: Applications of the stochastic YORP model. *Icarus* 247, 191-217.
- Brož, M., Thesis, 1999, Charles Univ., Prague, Czech Republic.
- Brož, M., Morbidelli, A. 2013. The Eos family halo. *Icarus*, 223, 844-849.
- Brož, M., Morbidelli, A., Bottke, W. F., Rozehnal, J., Vokrouhlický, D., Nesvorný, D. 2013. Constraining the cometary flux through the asteroid belt during the late heavy bombardment. *Astronomy and Astrophysics* 551, A117.
- Bus, S. J., Binzel, R. P. 2002a. Phase II of the Small Main-Belt Asteroid Spectroscopic Survey. The Observations. *Icarus* 158, 106-145.
- Bus, S. J., Binzel, R. P. 2002b. Phase II of the Small Main-Belt Asteroid Spectroscopic Survey. A Feature-Based Taxonomy. *Icarus* 158, 146-177.
- Carruba, V., Burns, J. A., Bottke, W., Nesvorný, D. 2003. Orbital evolution of the Gefion and Adeona asteroid families: close encounters with massive asteroids and the Yarkovsky effect. *Icarus* 162, 308-327.
- Carruba, V., Michtchenko, T. A. 2007. A frequency approach to identifying asteroid families. *Astronomy and Astrophysics* 475, 1145-1158.
- Carruba, V. 2009. The (not so) peculiar case of the Padua family. *Monthly Notices of the Royal Astronomical Society* 395, 358-377.

- Carruba, V. 2010. The stable archipelago in the region of the Pallas and Hansa dynamical families. *Monthly Notices of the Royal Astronomical Society* 408, 580-600.
- Carruba, V., Domingos, R. C., Nesvorný, D., Roig, F., Huaman, M. E., Souami, D. 2013. A multidomain approach to asteroid families' identification. *Monthly Notices of the Royal Astronomical Society* 433, 2075-2096.
- Carruba, V., Nesvorný, D., Aljbaae, S., Huaman, M. E. 2015a. Dynamical evolution of the Cybele asteroids. *Monthly Notices of the Royal Astronomical Society* 451, 244-256.
- Carruba, V., Nesvorný, D., Aljbaae, S., Domingos, R. C. 2015b,. On the oldest asteroid families in the main belt. *Monthly Notices of the Royal Astronomical Society*, submitted.
- Carruba, V., Nesvorný, D. 2015c. The Contribution of Ejection Speeds to the Inclination Distribution of Asteroid Family Members . *Monthly Notices of the Royal Astronomical Society*, in press.
- Carry, B. 2012. Density of asteroids. *Planetary and Space Science* 73, 98-118.
- Cellino, A., Dell'Oro, A., Zappalà, V. 2004. Asteroid families: open problems. *Planetary and Space Science* 52, 1075-1086.
- Cellino, A., Dell'Oro, A., Tedesco, E. F. 2009. Asteroid families: Current situation. *Planetary and Space Science* 57, 173-182.
- DeMeo, F. E., Carry, B. 2013. The taxonomic distribution of asteroids from multi-filter all-sky photometric surveys. *Icarus* 226, 723-741.
- Durda, D. D., Bottke, W. F., Nesvorný, D., et al. 2007, Size-frequency distributions of fragments from SPH/ N-body simulations of asteroid impacts: Comparison with observed asteroid families. *Icarus*, 186, 498-516.
- Hanuš, J., Brož, M., Ďurech, J., Warner, B. D., Brinsfield, J., Durkee, R., Higgins, D., Koff, R. A., Oey, J., Pilcher, F., Stephens, R., Strabla, L. P., Ulisse, Q., Girelli, R. 2013, An anisotropic distribution of spin vectors in asteroid families. *A&A* 559, A134.
- Ivezić, Ž., and 32 colleagues 2001. Solar System Objects Observed in the Sloan Digital Sky Survey Commissioning Data. *The Astronomical Journal* 122, 2749-2784.
- Knežević, Z., Milani, A., 2000, Synthetic Proper Elements for Outer Main Belt Asteroids, *Celestial Mechanics and Dynamical Astronomy*, 78, 17-46.
- Lazzaro, D., Angeli, C. A., Carvano, J. M., Mothé-Diniz, T., Duffard, R., Florczak, M. 2004. S<sup>3</sup>OS<sup>2</sup>: the visible spectroscopic survey of 820 asteroids. *Icarus* 172, 179-220.
- Masiero, J. R., Mainzer, A. K., Grav, T., et al. 2011. Main Belt Asteroids with WISE/NEOWISE. I. Preliminary Albedos and Diameters. *The Astrophysical Journal*, 741, 68-88.
- Masiero, J. R., Mainzer, A. K., Grav, T., Bauer, J. M., Jedicke, R. 2012. Revising the Age for the Baptistina Asteroid Family Using WISE/NEOWISE Data. *The Astrophysical Journal* 759, 14.
- Molnar, L. A., Haegert, M. J. 2009. Details of Recent Collisions of Asteroids 832 Karin and 158 Koronis. *AAS/Division for Planetary Sciences Meeting Abstracts* #41 41, #27.05.

- Morbidelli, A., Nesvorný, D. 1999. Numerous Weak Resonances Drive Asteroids toward Terrestrial Planets Orbits. *Icarus* 139, 295-308.
- Murray, C. D., Dermott, S. F. 1999. Solar system dynamics. Solar system dynamics by Murray, C. D., Cambridge Univ. Press.
- Nesvorný, D., Bottke, W. F., Jr., Dones, L., Levison, H. F. 2002. The recent breakup of an asteroid in the main-belt region. *Nature* 417, 720-771.
- Nesvorný, D., Enke, B. L., Bottke, W. F., Durda, D. D., Asphaug, E., Richardson, D. C. 2006. Karin cluster formation by asteroid impact. *Icarus* 183, 296-311.
- Nesvorný, D., Brož, M., Carruba, V. 2015. Identification and Dynamical Properties of Asteroid Families. ArXiv e-prints arXiv:1502.01628. In Asteroid IV, (P. Michel, F. E. De Meo, W. Bottke Eds.), Univ. Arizona Press and LPI, in press.
- Novaković, B., Clara, M., Tsirvoulis, G., Knežević, Z. 2015, Asteroid Secular Dynamics: Ceres Fingerprint Identified, *The Astrophysical Journal*, 807, L5.
- Tholen, D. J., 1989, Asteroid taxonomic classifications, IN: Asteroids II; Proceedings of the Conference, Tucson, AZ, Mar. 8-11, 1988 (A90-27001 10-91). Tucson, AZ, University of Arizona Press, 1989, p. 1139-1150.
- Vokrouhlický, D., Nesvorný, D., Bottke, W. F., 2003, The vector alignments of asteroid spins by thermal torques. *Nature*, 425, 147-151.
- Vokrouhlický, D., Brož, M., Morbidelli, A., Bottke, W. F., Nesvorný, D., Lazzaro, D., Rivkin, A. S. 2006. Yarkovsky footprints in the Eos family. *Icarus* 182, 92-117.
- Xu, S., Binzel, R. P., Burbine, T. H., Bus, S. J. 1995. Small main-belt asteroid spectroscopic survey: Initial results. *Icarus* 115, 1-35.
- Zappalà, V., Cellino, A., & Farinella, P. 1990, Hierarchical Clustering: How to Identify Asteroid Families and Assess their Reliability, Proceedings of a meeting (AMC 89) held at the Astronomical Observatory of the Uppsala University, June 12-16, 1989, Uppsala: Universitet, 1990, edited by C.I. Lagerkvist, H. Rickman, and B.A. Lindblad., p.211.
- Zappalà, V., Cellino, A., Dell'oro, A., Migliorini, F., Paolicchi, P. 1996. Reconstructing the Original Ejection Velocity Fields of Asteroid Families. *Icarus* 124, 156-180.
- Zellner, B., Tholen, D. J., Tedesco, E. F. 1985. The eight-color asteroid survey - Results for 589 minor planets. *Icarus* 61, 355-416.